Vokasi Unesa Bulletin of Engineering, Technology and Applied Science (VUBETA)
https://journal.unesa.ac.id/index.php/vubeta
Vol. 3, No. 1, 2026, pp. 88~101 DOI: 10.26740/vubeta.v3i1.44016
ISSN: 3064-0768

Design and Control of a Seaweed Dryer Prototype Powered by Solar and Wind Energy

Setiyono[1*], Elfitrin Syahrul[2], Dyah Nur'ainingsih[3]
[1,2,3]Department of Electrical Engineering, Faculty of Industrial Technology, Universitas Gunadarma, Jakarta, Indonesia

Article Info

Article history:

Received July 11, 2025
Revised October 8, 2025
Accepted December 15, 2025

Keywords:

Seaweed Dryer
Hybrid Power
Solar Panel
Wind Energy
XH-M609 Module

ABSTRACT

Seaweed drying is a crucial step in maintaining product quality and shelf life. However, conventional methods still face significant challenges, including high energy consumption, reliance on fossil fuels, and instability in quality due to environmental variability. This research developed a prototype hybrid-powered seaweed dryer that simultaneously utilizes solar and wind energy and is equipped with an automated control system to monitor and regulate temperature and humidity during the drying process. The prototype can operate in both manual and automatic modes, making it suitable for small-scale production and off-grid environments. Test results demonstrated that the prototype can effectively utilize hybrid renewable energy sources while maintaining adaptive protection and control based on environmental conditions, offering a cost-effective and environmentally friendly solution for small-scale seaweed farmers This article presents measurable results in the form of output voltage, current, and power generated by the solar panel and wind turbine, which demonstrate the capability of the hybrid energy system to supply power for the seaweed dryer. The novelty of this research lies in the integration of dual energy sources with an automated control system, which has not been widely implemented in previous seaweed dryers. This approach improves energy efficiency, lowers operational costs, and offers a sustainable solution for seaweed production, while supporting the development of environmentally friendly drying technologies.

1. INTRODUCTION

Seaweed is a fishery commodity with high economic value that is widely used in the food, pharmaceutical, cosmetic, and bioproduct industries due to its abundant polysaccharides, proteins, vitamins, and minerals [1]–[4]. Seaweed production in various coastal areas, including Indonesia, continues to increase in line with high global market demand. However, the main challenge in post-harvest is maintaining product quality, as the high water content (60–90%) makes it prone to microbiological and chemical degradation [5]–[7]. Therefore, an efficient and controlled drying process is crucial to extend shelf life and maintain nutritional quality [8]–[10].

Traditional drying methods, such as direct sun drying, are still commonly used by small-scale farmers but are highly weather-dependent, prone to contamination, and often produce inconsistent quality [11][12]. As an alternative, various studies have developed drying systems powered by solar, biomass, or electricity, equipped with temperature and humidity controls to improve efficiency and quality [13]–[16]. Wind energy, with its increasing share in the global energy mix, presents challenges of variability and intermittency that complicate grid integration [17]. Recent innovations have led to hybrid drying systems that use a combination of renewable energy sources, such as solar and wind, with a backup source (biomass or electricity) to ensure continuous operation [18]–[20]. The performance of hybrid dryers for seaweed has been shown to accelerate drying rates, reduce fossil fuel consumption, and reduce carbon emissions [21]–[25]. Several studies also show that integrating Photovoltaic/Thermal (PV/T) technology can provide heat and electrical energy simultaneously for the drying system [26]–[29].

*Corresponding Author
Email: setiyono@staff.gunadarma.ac.id

These dryer designs are usually equipped with intelligent controls based on the Internet of Things (IoT) to maintain temperature and humidity at optimal levels according to the characteristics of seaweed drying kinetics. It is added that IoT-based systems provide real-time data on renewable energy generation, thereby increasing the responsiveness and effectiveness of demand response strategies [30]-[39]. From an energy security perspective, power management is a crucial aspect of hybrid dryers operating in remote coastal areas. Optimizing the energy system size, load scheduling strategies, and multi-source management algorithms are the focus of recent research aimed at minimizing operational costs and maximizing renewable energy utilization [40]- [44]. In addition, mathematical modeling of the drying process and technical simulations help in designing prototypes with high thermal performance and energy efficiency [45]- [51].

This research contributes to the development of a hybrid seaweed dryer prototype equipped with an integrated control system for regulating the drying process and managing energy. Innovations include the mechanical design of the drying chamber, the configuration of the hybrid power source (PV and wind), and a real-time control algorithm that combines temperature and humidity sensor data with an energy optimization strategy. There has been no previous research in Indonesia that integrates two renewable energy sources (solar and wind) into a single seaweed drying system, implements an automatic control system based on environmental sensors to improve drying efficiency and product quality, provides smart battery protection to enhance the reliability of the hybrid system, and offers a quantitative comparison with conventional drying methods. The ultimate goal is to produce a prototype dryer that is efficient, sustainable, and adaptive to energy and environmental conditions, to support a reliable seaweed supply chain in remote coastal areas.

1.1 Solar Energy

Solar energy has a significant advantage: it can be directly used in residential settings, allowing each household to generate its own electricity with a Home Solar Power System [52]. A photovoltaic device converts solar energy into electrical energy. This device is a collection of solar cells arranged in series or parallel, forming a solar module. The number of solar panels (n) needed to design energy capacity can be determined by the equation:

$$n = \frac{Planned\ Power}{Power\ on\ PV} \tag{1}$$

The photovoltaic efficiency (η, PV) of a solar PV system is the ratio of solar energy converted to electrical energy and can be calculated using the equation.

$$\eta_{PV} = \frac{P_{max}}{P_{inc}} \tag{2}$$

P_{max} is the maximum output power of the photovoltaic, P_{inc} (P Incoming) is the power that goes into the solar panel module. The instantaneous power produced by a PV system (kW) can be determined using the equation:

$$P_{PV,t} = C_{PV}\eta_{PV}\left(\frac{G_{T,t}}{G_{T,STC}}\right)\left(1 + \alpha_p(T_{C,t} - T_{C,STC})\right) \tag{3}$$

C_{PV} PV array (kW), η_{PV} is an efficiency (%), $G_{T,t}$ t is solar radiation (kW/m2), $G_{T,STC}$ is solar radiation in (kW/m2) on standard test conditions of solar temperature (STC), α_P is PV cell temperature power coefficient (%/0C), $T_{C,t}$ solar cell temperature (00C), $T_{C,STC}$ solar cell temperature in STC (standard test condition) mode.

1.2 Wind Energy

The use of wind energy worldwide has increased rapidly in recent years to reduce greenhouse gas emissions [53]-[54]. To convert it into electrical energy, a wind turbine is needed, which converts wind speed into angular rotation to rotate a generator. The equation can represent the amount of mechanical power of a wind turbine:

$$P_{Wind} = \frac{1}{2}\rho A V^3 C_p \tag{4}$$

where P_{Wind} is the wind turbine output power, ρ is the air density, V is the wind velocity, Cp is the turbine's coefficient of energy.

1.3 DC Generator

This research uses a 300-W DC engine generator to charge batteries without requiring an AC-DC converter. It uses a permanent-magnet DC generator to generate more power. A permanent magnet generator

has high efficiency at low rotation speeds. Cross-flow turbines work perfectly on a discharge that is not too high. Mostly, micro hydro power plants use DC generators. It uses water power as its propulsion. This small-scale micro hydro generator can produce 270 watts with a voltage output of 12 -18 Volts.

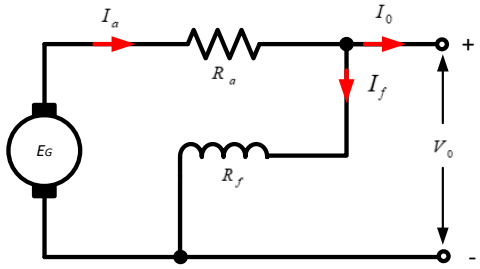

Figure 1. DC Shunt Generator

The KVL circuit equation presented in Figure 1 can be written as follows:

$$E_G = I_a R_a + V_0 \tag{5}$$

$$E_G = kn\phi \tag{6}$$

$$I_a = I_f + I_0 \tag{7}$$

$$V_0 = kn\phi - I_a R_a \tag{8}$$

$$V_0 = I_f R_f \tag{9}$$

Where E_G (Electrical Motion Force, emf), R_a (Resistance armature), R_f (Resistance field), I_a (armature current), I_f (field current), I_0 (Load current), V_0)(output voltage), ϕ (flux), n (generator speed). Equation 8 shows that the output voltage value can be adjusted by increasing the speed and adjusting the armature current or field current.

2. METHOD

This research follows a four-stage methodology to develop and evaluate a hybrid solar-wind seaweed dryer. First, the research design adopts an experimental prototype approach with comparative performance analysis. Next, in system development, key components—solar panels, wind turbines, battery storage, inverter, controller, and drying chamber—are integrated and monitored for energy input. The experimental procedure involves drying trials under four modes: solar-only, wind-only, hybrid, and conventional sun drying. Finally, the evaluation and analysis stage compares drying efficiency, energy usage, and system responsiveness to assess the viability of renewable-powered drying solutions, as seen in Figure 2.

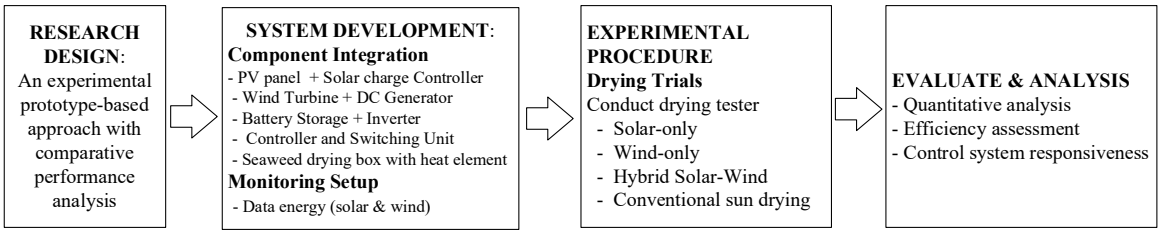

Figure 2. System Seaweed Dryer Flowchart

This study adopts an experimental prototype-based design to develop and evaluate a hybrid solar–wind powered seaweed dryer. The system integrates photovoltaic panels, a wind turbine with a DC generator, battery storage, an inverter, a control unit, and a heat-assisted drying chamber. A monitoring setup tracks solar irradiance, wind speed, voltage, current, battery charge, and chamber temperature and humidity. Measurements using digital multimeters and power meters were conducted under varying weather and wind conditions to assess energy output and system stability. The prototype was built using electronic hardware and tested through operational trials, with solar and wind energy used alternately to power the dryer. Collected data were analyzed to evaluate the efficiency and reliability of the hybrid energy system in supporting seaweed drying.

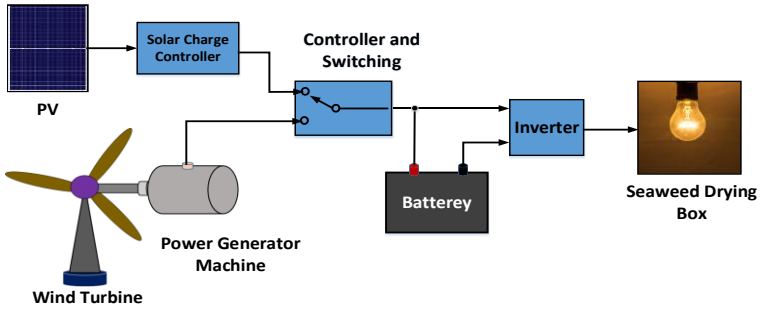

Figure 3. Hybrid Powered Seaweed Dryer System

Figure 3 illustrates the dual power sources—solar and wind—used to charge the battery via a comparator circuit and a solar charge controller (SCC). The SCC acts as a switch, selecting the higher input voltage for charging while protecting against overcharge and discharge. The battery stores energy from both sources, which is then converted by an inverter from 12V DC to 220V AC. The final output powers a drying box equipped with a heating element and fan for air circulation. A rain sensor automatically controls the protective roof during rainfall. Figure 4 shows the seaweed dryer prototype, while Figure 5 presents the wiring layout of all components.

Figure 4. Prototype of Seaweed Dryer.
[1: Solar cell; 2: Wind Turbine and DC Generator Set; 3: controller; 4: battery; 5: drying box]

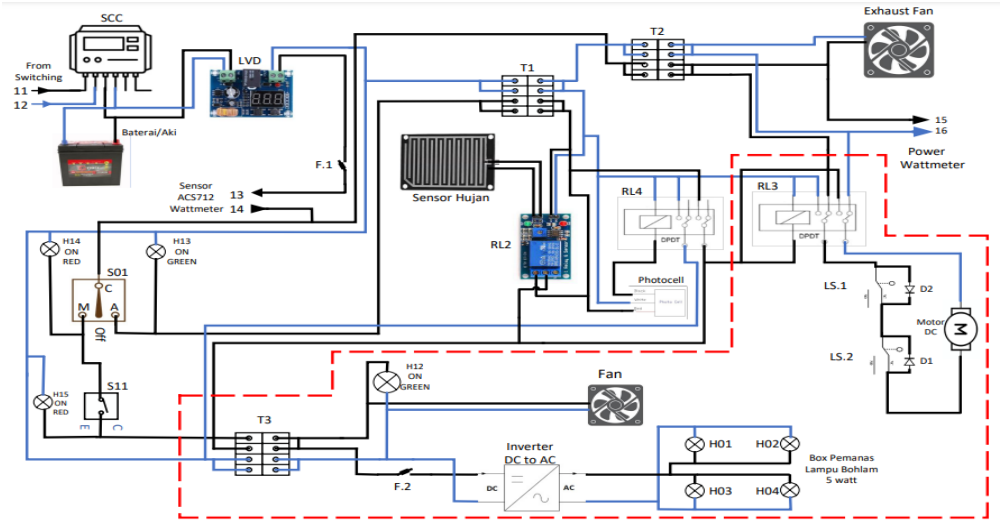

Figure 5. Electrical Wiring Diagram of Seaweed Dryer System

3. RESULTS AND DISCUSSION

This section explains the two energy sources powering the prototype system being built. Two power sources are connected in a hybrid manner and work alternately to charge the battery depending on which voltage is greater, between the wind energy and solar energy sources.

3.1 Solar Power System Testing

Solar energy is used to dry seaweed during the day, from 07.00 A.M. to 5.00 P.M., for approximately 10 hours. Photovoltaics use sunlight to charge the battery. The type of solar panel used in this research is a 36-cell monocrystalline module. Technical data for the solar module is shown in Table 1.

Table 1. Parameter Technical Solar Panel PMS 30 Wp

Maximum Power (Pmax)	30Wp
Maximum Power Voltage (Vmpp)	18 V
Maximum Power Current (Impp)	1,67 A
Open Circuit Voltage (Voc)	22.5 V
Short Circuit Current (Isc)	1.8 A
Power Tolerance(Positive)	5%
Module Efficiency STC	14.23%
Operating Temperature Range	-40°C to +85°C
Maximum System Voltage	715V
Series Fuse Rating	8A
Temperature Coefficient of Pmax	-0.44 %/°C
Temperature Coefficient of Voc	-0.33 %/°C
Temperature Coefficient of Isc	0.055 %/°C
Nominal Operating Cell Temperature(NOCT)	45±2°C

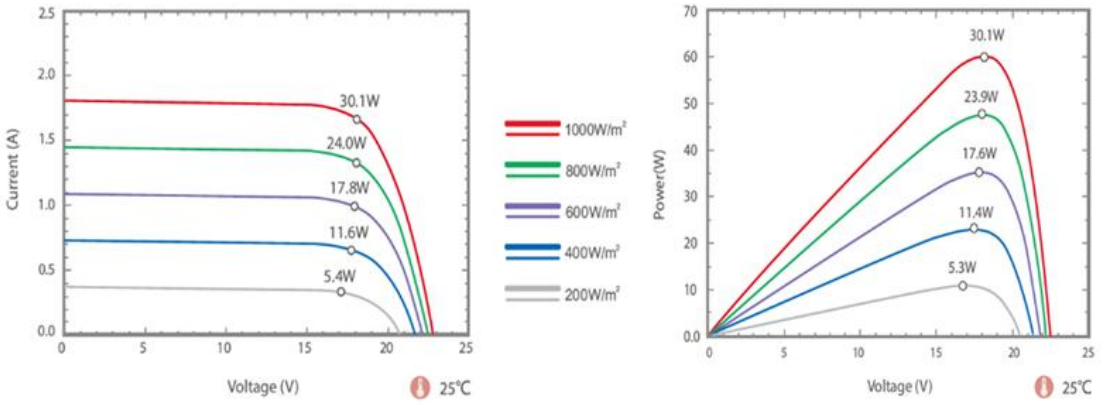

(a) (b)

Figure 6(a)Voltage and Current Characteristics Curves. Figure 6(b)Voltage and Power Characteristics Curves

Figure 6(a) shows the V/I solar panels' characteristics—the maximum current in short circuit condition ±1.8 A on irradiation level around 1000 W/m^2. Maximum power of approximately 30.1 W was obtained with current (I) and voltage (V) values around ±1.6 A and ±18 V, respectively. Figure 6(b) shows that the power curve has a maximum power point (MPP). The maximum power point voltage (V_{mpp}) is less than the open circuit voltage. The current MPP (I_{mpp}) is lower than the short circuit current. The maximum power and efficiency of solar cells decrease as temperature increases. In general, increasing the temperature from 25ºC results in a power reduction of around 10%.Solar panel testing is performed to determine the voltage output of the solar panel. Battery charging is regulated by the solar charge controller (SCC). Table 2 shows the results of observations conducted over 11 hours from 07.00 am to 5.00 pm. Data collection was carried out 11 times, with a 1-hour break (60 minutes) between each.

Table 2. Solar Panel Testing

Time	Voltage (Volt)	Weather
07.00 a.m	12.05	Sunny
08.00 a.m	12.10	Sunny
09.00 a.m	13.52	Sunny
10.00 a.m	14.27	Cloudy
11.00 a.m	14.20	Cloudy

Time	Voltage (Volt)	Weather
12.00 a.m	15.53	Sunny
1.00 p.m	15.68	Sunny
2.00 p.m	15.55	Sunny
3.00 p.m	14.61	Sunny
4.00 p.m	13.80	Sunny
5.00 p.m	12.23	Sunny

The average temperature, whether sunny or cloudy, is ±33°C. The highest voltage is in Table 4.3. obtained at 13.00 or 1 pm at 15.68V, and the lowest voltage obtained at 07.00 or 7 am at 12.05V. When the weather is cloudy, the voltage produced by the solar panels is around 14.27V at 10.00 and 14.20V at 11.00.

3.2 Wind Power System Testing

A low RPM permanent Magnet Generator can produce electricity at 400 rpm, around 16 Volts. As a wind power generator simulator, a fan with a blade length of 16 inches (40 cm), 220 V, 50 Hz, 50 W, and adjustable rotational speed control is used.

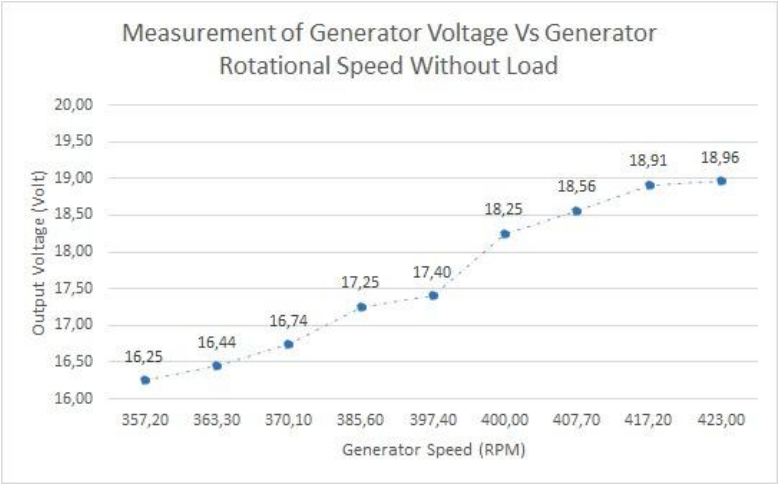

Figure 7. Measurement of Generator Voltage versus Generator Rotational Speed Without Load

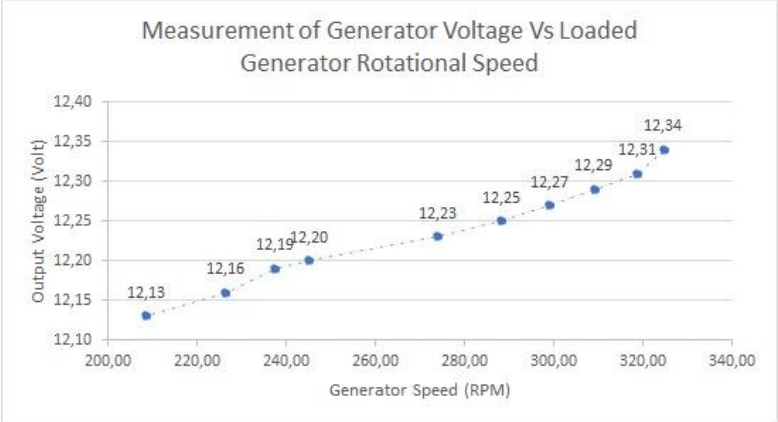

Figure 8. Measurement of Generator Voltage vs Loaded Generator Rotational Speed

From Figures 7 and Figure 8, it can be concluded that weather changes directly affect the voltage generated by the hybrid power system combining wind and solar panels. During clear weather, high sunlight intensity increases the solar panel's output, resulting in optimal voltage generation. Conversely, during cloudy or rainy conditions, reduced sunlight intensity reduces the voltage produced by the solar panel. In this situation, the wind turbine can serve as the primary energy source, with its voltage output depending on wind speed. If the wind speed is high, the generated voltage remains stable and can compensate for reduced solar panel output. However, during severe weather conditions with low sunlight intensity and weak wind, the total voltage of the hybrid system will drop significantly. Thus, voltage fluctuations occur due to weather variability, where both energy sources work together to maintain a continuous power supply.

3.3 Control System Testing (Auto and Manual)

This prototype is designed to operate in two modes: automatic and manual. Automatic mode testing of the tool is performed by running the system both automatically and manually. The components tested include switches, relays, two sensors, namely a photocell sensor and a raindrop sensor as automatic input, and indicator lights.

3.3.1 Automatic Mode

Testing the tool is based on Table 5: when the system switch is in the OFF condition, the current from the source to the load is not connected. Even though the manual switch is ON, the photocell sensor and the raindrop sensor both receive triggers. Because the electric current is not connected, the DC motor relay and load indicator will be OFF. When the system switch is in manual mode, the current from the source to the load is connected. If the manual switch is ON, the DC motor relay and load indicator will be ON; if it is OFF, the electric current will not be connected to the load. Likewise, when the system is operated manually, if one of the sensors is triggered, the system will not supply current from the source to the load, and the DC motor and load indicator will be OFF because the system is operated manually via a manual switch. When the system switch is in automatic mode, the current from the source to the load will flow if either or both sensors are ON. When the photocell sensor is ON, the DC motor and load indicator will be ON. Then, when the raindrop sensor is ON, the DC motor and load indicator will be ON Likewise, when both sensors are ON, the DC motor and load indicator will be ON. Meanwhile, if both sensors are OFF, the system will not distribute electric current from the source to the load. Likewise, if the manual switch is ON, the DC motor relay and load indicator will be OFF, as the system operates automatically with the sensor as the switch.

Table 5 . Switches and sensors status in automatic operation mode

Switch Sistem			Manual Switch	Sensor		Relay	Indicator
I	0	II		Photocell	Raindrop	DC Motor	Load
X	O	X	OFF	OFF	OFF	OFF	OFF
X	O	X	OFF	ON	OFF	OFF	OFF
X	O	X	OFF	OFF	ON	OFF	OFF
X	O	X	ON	OFF	OFF	OFF	OFF
O	X	X	OFF	OFF	OFF	OFF	OFF
O	X	X	OFF	ON	OFF	OFF	OFF
O	X	X	OFF	OFF	ON	OFF	OFF
O	X	X	ON	OFF	OFF	ON	ON
X	X	O	OFF	OFF	OFF	OFF	OFF
X	X	O	OFF	ON	OFF	ON	ON
X	X	O	OFF	OFF	ON	ON	ON
X	X	O	ON	OFF	OFF	OFF	OFF
X	X	O	OFF	ON	ON	ON	ON

Description Table 5, as follows :
I = The system works manually
0 = System is not active or OFF
II = The system works automatically
O = Condition used
X = Unused condition

3.3.2 Manual Mode

In manual operation mode, the switch response is carried out to determine the response time required for the manual switch to disconnect and connect electrical current.

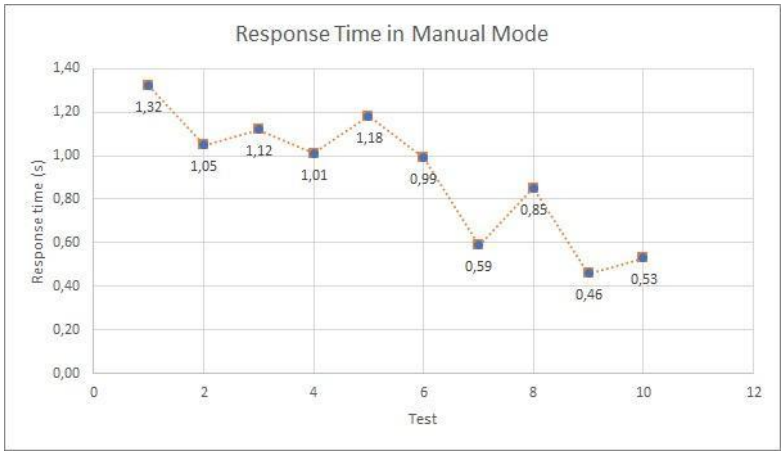

Figure 9. Testing the Response Time of the Manual Mode Switch Operation

Figure 9 shows the results of testing the manual switch response to the system. This response-time test uses a stopwatch to measure the switch's response time. Based on Table 5, it is found that the manual switch response time from the initial OFF condition to the final ON condition was 1.32s (seconds) in the first experiment, 1.05s (seconds) in the second experiment, 1.12s (seconds) in the third experiment, and 1.12s (seconds) in the fourth experiment. Amounted to 1.01s (seconds), and in the fifth experiment, it was 1.18s (seconds). Furthermore, the results of testing the manual switch response time from the initial ON condition to the final OFF condition were in the first experiment, it was 0.99s (seconds); in the second experiment, it was 0.59s (seconds), in the third experiment, it was 0.85s (seconds), in the fourth experiment, it was 0.85s (seconds). 0.46s (seconds) and in the fifth experiment, it was 0.53s (seconds). Based on all the experiments carried out, the system is functioning.

3.3.3 Automatic Switch Control

The selector switch connects the battery to the voltage source that will charge it, based on the voltage level of the two power sources (WPP or SPP), using a comparator and relay circuit. In testing the comparator circuit, the aim is to determine the input voltage from WPP and SPP, the voltage at pin 2 (SPP input voltage), the input voltage at pin 3 (WPP input voltage), the input voltage at pin 6 (output) of IC LM741, the condition of the indicator light when WPP>SPP and when SPP>WPP, and the relay conditions when WPP>SPP and when SPP>WPP.

Table 6. Measurements and Conditions in the Comparator Circuit

Source	Vin (V)	Voltage on IC LM741			The power Generator that charges the battery
		Pin 2 (V)	Pin 3 (V)	Pin 6 (V)	
SPP	13.55	6.08	-	0.013	SPP
WPP	11.40	-	5.46		
SPP	11.58	5.80	-	9.98	WPP
WPP	12.68	-	6.11		

WPP : Wind Power Plant , SPP : Solar Power Plant

Table 6 shows the measurements and conditions in the comparator circuit. The voltage at pin 2 (SPP input voltage) of the LM741 IC is not the same as the input from the solar panel because the comparator circuit includes a voltage divider. The voltage at pin 3 (WPP input voltage) of the LM741 IC is not the same as the input voltage of the WPP. This is because the comparator circuit includes a voltage divider. When the SPP voltage > WPP, the LM741 IC's pin 6 (output) voltage is 0.013V, which turns off the indicator light and keeps the relay in NC, which is connected to the SPP and charges the battery using electrical energy produced by the SPP. When the WPP > SPP voltage, the voltage at pin 6 of the LM741 IC is 9.98V, which turns on the indicator light and moves the relay to the NO position, which is connected to the WPP and charges the battery using the electrical energy produced by the WPP.

3.3.4 Battery, Inverter, and Drying Box

Batteries are used to store electrical charge from deep-cycle solar panels, VRLA AGM, or VRLA Gel types. This battery performs well in charging cycles and use, is leak-proof, and is maintenance-free. Battery

capacity 12 V 70 Ah. So this battery can provide 12V x 70 Ah = 840 Wh. This means that in 1 hour, it can deliver 840 Watts of power. The inverter converts direct battery voltage to alternating voltage to power the heater in the dryer box unit. This inverter is in the form of a 2×2-switch circuit (4 switches), wired in parallel and designed to work in complementary pairs. This inverter switch ignition circuit was selected using the Sinusoidal Pulse Width Modulation (SPWM) method. The output waveform is a series of square pulses. This voltage still contains harmonic content, so a filter is needed to reduce its distortion. As shown in Figure 5, the overall circuit of the Seaweed Dryer Box with the Hybrid Power System works as follows: when the battery or accumulator power source is connected, the current flows to the control system. Then, from the control system, the current flows to the terminal (T3). This terminal (T3) is the main terminal for activating the components for the load in use. When the terminal (T3) receives electric current from the control system, it flows to each load. The first load is the fan on the dryer box when the terminal (T3) receives electric current. Meanwhile, the electric current goes to the fuse (F2) and then to the inverter. This inverter converts DC (direct current) to AC (alternating current). After that, the AC electric current from the inverter powers the incandescent lamp and activates all the lights on the dryer box. The DC motor opens and closes the dryer box. When the DC motor relay is not active, the current that flows through the normally close (NC) contact of the relay will be connected to the DC motor, and with the polarity reversed between positive and negative, then open the dryer box, but the positive electric current that goes to the DC motor will go through the limit switch first. In this device, limit switches are installed in series when current passes through both limit switches 1 and 2. When limit switch 2 is touched, the DC motor will no longer open, so the current through the DC motor is cut off because the previous limit switch contact is normally closed. (NC) changes to normally open (NO), and in the limit switch, a reverse-bias diode is installed between the common (COM) and normally closed (NC) contacts so that it cannot flow to the DC motor. Meanwhile, if limit switch 1 is pressed, the DC motor will not stop opening the drying box because in limit switch 1, a diode is installed between the common (COM) and normally close (NC) in a forward bias manner, so that if limit switch 1 is pressed, electric current will continue to flow towards the DC motor.

Then, when the DC motor relay is active, the current flowing through the normally open (NO) relay contact will be connected to the DC motor, and with the polarity reversed between positive and negative, then close the dryer box, but the negative electric current going to the DC motor will go through the limit switch first. In this device, limit switches are installed in series when current passes through both limit switches 1 and 2. When limit switch 1 is touched, the DC motor will not close again, so the current through the DC motor is cut off because the previous limit switch contact is normally closed. (NC) changes to normally open (NO) and in limit switch 2, a reverse bias diode is also installed between the common (COM) and normally closed (NC) contacts so that it cannot flow to the DC motor. Meanwhile, if limit switch 2 is pressed, the DC motor will not stop closing the drying box because in limit switch 2 a diode is installed between the common (COM) and normally close (NC) in a forward bias manner so that if limit switch 2 is pressed, electric current will continue to flow towards the DC motors. When the load is connected to an electrical source, the load indicator will light up. The flow diagram illustrates how the seaweed drying box operates with a hybrid power system. The diagram of a seaweed-drying box with a hybrid power system is shown in Figure 10.

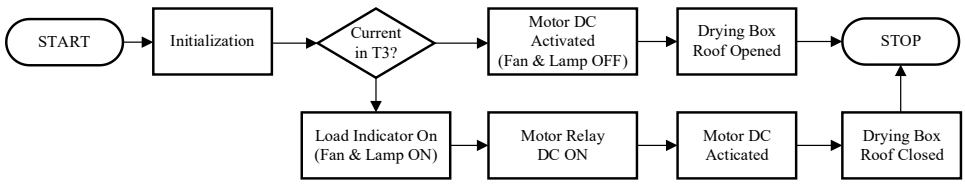

Figure 10. Seaweed Dryer's Flow Diagram using Hybrid Power System

Figure 10 is a flow diagram of a seaweed drying box with a hybrid power system. The flow diagram presented depicts a series of steps in a process with clear stages. The process begins with the "Device Initialization" step, during which all devices involved are prepared and configured according to requirements. Next, the system performs an "Electric Current Check at Terminal (T3)" with two possible results. If the check results show that the terminal (T3) is not receiving electric current, the system will take the following action: "DC Motor Is On, and Fan Is Not On". At this stage, the DC motor is turned on, but the fan remains inactive. Followed by "Opening the Dryer Box". Then, if the check results show that the terminal (T3) is receiving electric current, the system takes a different course of action. "Load, Fan, and Light Indicators On" indicates that the system provides visual signals for the status of the electrical load, fans, and lights. Next, "DC Motor Relay Turns On and DC Motor Moves" activates the DC motor relay, enabling the motor to start moving according to the system design. After that, "Box Closing". These two paths lead to the "Process Complete" step, which indicates that the primary process has been completed and the flow diagram ends. In the overall

context, this flow diagram illustrates how the system responds to the status of the electrical current at the terminal (T3), with a series of planned actions depending on the check results.

The load on the drying box consists of an incandescent lamp, which is helpful as a heater, a fan as a dryer, and a DC motor, which opens and closes automatically, as seen in Table 7.

Table 7. Load on Seaweed Dryer Box

Load	Calculated Power (W)	Rated Power (W)
Fan 2 W + 10 W Bulb	12	47.1
Fan 2 Watt + 20 W Bulb	22	75.7
Fan 2 Watt + 30 W Bulb	32	107.2
Fan 2 Watt + 40 W Bulb	42	137.8

The load test results were 47.1W for the fan load and 208.1VAC at the inverter output when the inverter input voltage was 12.07V. Then, with a load specification power of 12W, the power used was 47.1W with a battery supply time of 12 hours and 58 minutes. Then the fan load and two incandescent lamps with DC power obtained are 75.7W, and the inverter output obtained is 205.5V when the inverter input voltage is 11.80V. Then, with a load specification power of 22W, the power used is 75.7W, with a battery supply time of 7 hours and 54 minutes. Then, with a fan load and three incandescent lamps powered by DC, 107.2W was measured, and the inverter output was 202.3VAC at an inverter input voltage of 11.80V. Then, with a load specification power of 32W, the power used is 107.2W over time. The battery supplies 5 hours 47 minutes. With a fan load and four incandescent lamps powered by DC, the load is 137.8W, and the inverter output is 200Vac when the inverter input voltage is 10.81V. With a load specification power of 42W, the power used is 137.8W with a battery supply time of 3 hours 43 minutes. Based on the results of this operation, the tool can be concluded to work as intended.

3.4 Discussion

The experimental results demonstrated that the hybrid solar-wind-powered seaweed dryer prototype successfully operated using two renewable energy sources. The system alternated between solar and wind power based on each source's availability. The solar panel performance showed a maximum voltage of 15.68 V at 13:00 under sunny conditions, while the wind turbine system achieved a peak output of 18.96 V at a rotational speed of 423 RPM without a load. These results indicate that both energy sources are sufficient to charge the battery and supply continuous power to the drying system. However, variations in weather conditions affected energy output, highlighting the need for an intelligent control system to optimize switching and balance energy storage. The control system tests for both manual and automatic operation modes showed stable performance. The manual switch exhibited response times ranging from 1.01 to 1.32 seconds to connect the load and 0.46 to 0.99 seconds to disconnect it. In automatic mode, the integrated photocell and raindrop sensors successfully managed operations by enabling the system to function during appropriate daylight conditions and to stop during rainfall, thereby preventing rehydration of the seaweed.

This automation feature offers a significant advantage over conventional drying methods, which rely heavily on labor and are susceptible to unpredictable weather. Although the prototype testing was limited to system functionality without actual seaweed-drying trials, the temperature and humidity data suggest that the dryer has the potential to achieve the required drying conditions for seaweed, typically 40–60 °C. Compared to traditional open-air sun drying, which requires extended periods and large working areas, the hybrid system can potentially reduce drying time and improve product hygiene by operating in a controlled environment. Furthermore, the use of renewable energy minimizes operational costs and contributes to sustainable practices, especially for remote coastal communities with limited access to electricity. Future developments are essential to enhance the prototype's performance and adaptability. Integration with Internet of Things (IoT) platforms could allow real-time monitoring of drying parameters such as temperature, humidity, and energy levels, enabling farmers to supervise the process using mobile devices remotely. Moreover, advanced automatic control systems based on artificial intelligence or fuzzy logic could optimize power-source switching and heating-element operation, thereby improving energy efficiency and extending battery lifespan. Design improvements, such as weather-resistant and portable structures, would increase durability and usability in harsh coastal environments. Subsequent studies should focus on field trials using actual seaweed samples to evaluate the system's impact on drying efficiency, final moisture content, and product quality parameters, including color, texture, and nutrient retention. Additionally, scaling up the system with higher-capacity

batteries or supercapacitors would ensure continuous operation during nighttime or prolonged unfavorable weather conditions.

From a socio-economic perspective, the hybrid seaweed dryer has the potential to benefit coastal farming communities significantly. By reducing dependency on traditional sun drying, the system could enhance productivity, improve product quality, and increase market competitiveness. Community-based models, where groups of farmers collectively operate and maintain shared dryer units, could further reduce costs and promote cooperative economic development. If developed into an affordable commercial product, this technology could play a crucial role in empowering small-scale seaweed farmers and supporting sustainable aquaculture practices in Indonesia and beyond.

4. CONCLUSION

The prototype seaweed dryer powered by a hybrid power system has been completed and is operating well. In hybrid power plants, after testing, the following conclusions can be drawn: The maximum output voltage without load of the DC generator is the largest in the wind power plant (WPP) without load with a generator rotational speed of 423.0 RPM of 18.96V and the smallest voltage produced by the WPP without load with a generator rotational speed of 344.4RPM is 16.06V, Meanwhile, when the generator is under load, the maximum output voltage is 12.34V and the smallest voltage produced by WPP with a battery with a generator rotation speed of 208.7 RPM is 12.13V. The highest voltage measured from a 30 Wp solar panel (Watts peak) in this test was 15.68V at 13.00 or 1 pm, and the lowest was 12.05V at 07.00 or 7 am. In manual mode, when the manual switch is pressed, the current from the source is directly connected to the load. In automatic mode, when the system switch is in the auto position, and the raindrop and photocell sensors are triggered to ON, the current from the source will be connected to the load. Meanwhile, the system will not operate when the system switch is in the OFF state. The results of manual switch response tests on the system showed that the switch response time for connecting electric current was 1.01s to 1.32s, and for disconnecting electric current, 0.46s to 0.99s. Because this research is still at the prototype and device operation stage and has not yet progressed to testing with actual seaweed-drying objects, it remains highly open to further study. This research can be further developed into a fully functional device for testing the effectiveness, efficiency, and quality of seaweed drying.

ACKNOWLEDGEMENTS

Our deepest gratitude to Gunadarma University, especially the Electrical Engineering Department for their support and input to this research. We hope to pursue this research, therefore we could help seaweed farmer communities, especially on the seaweed drying process.

REFERENCES

[1] S. Suherman, H. Rizki, N. Rauf, & E. Susanto, "Performance Study of Hybrid Solar Dryer with Auxiliary Heater for Seaweed Drying", *Journal of Physics: Conference Series*, vol. 1295, no. 1, pp. 012002, 2019. https://doi.org/10.1088/1742-6596/1295/1/012002

[2] A. Suwandi, A. Fachrudin, & D. Setyanto, "Design of a Seaweed Draining and Drying Machine Using Hybrid Energy", *Jurnal Asiimetrik: Jurnal Ilmiah Rekayasa & Inovasi*, pp. 133-148, 2025. https://doi.org/10.35814/asiimetrik.v7i2.8636

[3] W. Agustiono, F. Wahyu, & W. Findiastuti, "An Internet of Things-based Solar Dryer: A Conceptual Design for Seaweed Cultivation in Madura", *BIO Web of Conferences*, vol. 146, pp. 01032, 2024. https://doi.org/10.1051/bioconf/202414601032

[4] H.-K. Phang, C.-M. Chu, S. Kumaresan, M. M. Rahman, & S. M. Yasir, "Preliminary Study of Seaweed Drying under A Shade and in A Natural Draft Solar Dryer", *International Journal of Science and Engineering*, vol. 8, no. 1, pp. 10–14, 2015. doi: https://doi.org/10.12777/ijse.8.1.10-14

[5] R. Sánchez, I. Kougias, M. Moner-Girona, F. Fahl, & A. Jäger-Waldau, "Assessment of Floating Solar Photovoltaics Potential in Existing Hydropower Reservoirs in Africa", *Renewable Energy*, vol. 169, pp. 687-699, 2021. https://doi.org/10.1016/j.renene.2021.01.041

[6] A. Naigam, I. Ridzuan, A. Tan, A. Abdullah, W. Ismail, & J. Janaun, "Design, Development and Performance Evaluation of a Large-Scale Hybrid Solar Dryer", *IOP Conference Series: Materials Science and Engineering*, vol. 1070, no. 1, pp. 012016, 2021. https://doi.org/10.1088/1757-899x/1070/1/012016

[7] E. Elangovan and S. Natarajan, "Experimental Study on Drying Kinetics of Ivy Gourd using Solar Dryer", *Journal of Food Process Engineering*, vol. 44, no. 7, 2021. https://doi.org/10.1111/jfpe.13714

[8] P. Chen, W. Chen, C. Lee, & J. Wu, "Comprehensive Review of Crystalline Silicon Solar Panel Recycling: From Historical Context to Advanced Techniques", *Sustainability*, vol. 16, no. 1, pp. 60, 2023. https://doi.org/10.3390/su16010060

[9] A. Rehman, M. Iqbal, M. Bhopal, M. Khan, F. Hussain, J. Iqbal et al., "Development and Prospects of Surface Passivation Schemes for High-Efficiency C-Si Solar Cells", *Solar Energy*, vol. 166, pp. 90-97, 2018. https://doi.org/10.1016/j.solener.2018.03.025

[10] R. Parthiban and P. Ponnambalam, "An Enhancement of the Solar Panel Efficiency: A Comprehensive Review", *Frontiers in Energy Research*, vol. 10, 2022. https://doi.org/10.3389/fenrg.2022.937155
[11] B. Merzah, Z. Al-Makhyoul, A. Abdullah, S. Ayed, & H. Majdi, "Enhancing Solar Panel Cooling and Thermal Efficiency Using Nanoparticle-Enhanced Phase Change Materials", *Mathematical Modelling of Engineering Problems*, vol. 11, no. 6, pp. 1547-1557, 2024. https://doi.org/10.18280/mmep.110615
[12] G. Granata, P. Altimari, F. Pagnanelli, & J. Greef, "Recycling of Solar Photovoltaic Panels: Techno-Economic Assessment in Waste Management Perspective", *Journal of Cleaner Production*, vol. 363, pp. 132384, 2022. https://doi.org/10.1016/j.jclepro.2022.132384
[13] F. Hajiahmadi, M. Jafari, & M. Reyhanoglu, "Machine Learning-Based Control of Autonomous Vehicles for Solar Panel Cleaning Systems in Agricultural Solar Farms", *AgriEngineering*, vol. 6, no. 2, pp. 1417-1435, 2024. https://doi.org/10.3390/agriengineering6020081
[14] H. Shin, K. Khoshelham, K. Lee, S. Jung, D. Kim, & W. Lee, "Effect of Incidence Angle on Temperature Measurement of Solar Panel with Unmanned Aerial Vehicle-Based Thermal Infrared Camera", *Remote Sensing*, vol. 16, no. 9, pp. 1607, 2024. https://doi.org/10.3390/rs16091607
[15] S. Khan, S. Chakraborty, K. Dash, A. Dar, F. Shawl, S. Dash et al., "Review of Solar Greenhouse Drying Systems in Conjunction with Hybrid Technological Features, Designs, Operations, and Economic Implications for Agro-Food Product Processing Application", *Energy Technology*, vol. 12, no. 8, 2024. https://doi.org/10.1002/ente.202400176
[16] S. Hidayat, K. Shabiya, S. Kadiran, I. Mujahidin, M. Prabowo, A. Nursyahid et al., "Real-Time Web-Based Monitoring System for Temperature, Humidity, and Solar Panels in Ramie Drying Facilities", *Scientific Journal of Informatics*, vol. 11, no. 1, pp. 69-80, 2024. https://doi.org/10.15294/sji.v11i1.47234
[17] A. Sabo, D. Dahiru, & N. Wahab, "A Modelling and Simulation of Damping Controller In DFIG AND PMSG Integrated With A Convectional Grid: A Review", *Vokasi Unesa Bulletin of Engineering, Technology and Applied Science*, vol. 2, no. 2, pp. 148-174, 2025. https://doi.org/10.26740/vubeta.v2i2.34749
[18] D. Sadeghi, N. Amiri, M. Marzband, A. Abusorrah, & K. Sedraoui, "Optimal sizing of hybrid renewable energy systems by considering power sharing and electric vehicles", International Journal of Energy Research, vol. 46, no. 6, p. 8288-8312, 2022. https://doi.org/10.1002/er.7729
[19] D. Rekioua, Z. Mokrani, K. Kakouche, A. Oubelaid, T. Rekioua, M. Alhazmi et al., "Coordinated Power Management Strategy for Reliable Hybridization of Multi-Source Systems using Hybrid MPPT Algorithms", *Scientific Reports*, vol. 14, no. 1, 2024. https://doi.org/10.1038/s41598-024-60116-4
[20] D. Rekioua, Z. Mokrani, K. Kakouche, T. Rekioua, A. Oubelaid, P. Logerais et al., "Optimization and Intelligent Power Management Control for An Autonomous Hybrid Wind Turbine Photovoltaic Diesel Generator with Batteries", *Scientific Reports*, vol. 13, no. 1, 2023. https://doi.org/10.1038/s41598-023-49067-4
[21] A. Krishna, A. Kumar, A. Krushna, J. Shanmugapriyan, & C. Keertana, "The Study of Solar and Wind Power Systems under Different Weather Conditions", *E3S Web of Conferences*, vol. 547, pp. 03009, 2024. https://doi.org/10.1051/e3sconf/202454703009
[22] A. Bazzi, H. Hafdaoui, A. Khallaayoun, K. Mehta, K. Ouazzani, & W. Zörner, "Optimization Model of Hybrid Renewable Energy Generation for Electric Bus Charging Stations", *Energies*, vol. 17, no. 1, pp. 53, 2023. https://doi.org/10.3390/en17010053
[23] T. Pop, C. Ungureanu, R. Pentiuc, C. Afanasov, V. Ifrim, P. Atănăsoaeet al., "Off-Grid Hybrid Renewable Energy System Operation in Different Scenarios for Household Consumers", *Energies*, vol. 16, no. 7, pp. 2992, 2023. https://doi.org/10.3390/en16072992
[24] A. Khamees, A. Abdelaziz, M. Eskaros, M. Attia, & M. Sameh, "Optimal Power Flow with Stochastic Renewable Energy Using Three Mixture Component Distribution Functions", *Sustainability*, vol. 15, no. 1, pp. 334, 2022. https://doi.org/10.3390/su15010334
[25] A. Mohammed, C. Komolafe, & A. Simons, "Advances in Solar Drying Technologies: A Comprehensive Review of Designs, Applications, and Sustainability Perspectives", *Solar Compass*, vol. 17, pp. 100153, 2025. https://doi.org/10.1016/j.solcom.2025.100153
[26] M. Hiloidhari, V. Vijay, R. Banerjee, D. Baruah, & A. Rao, "Energy-Carbon-Water Footprint of Sugarcane Bioenergy: A District-Level Life Cycle Assessment in the State of Maharashtra, India", *Renewable and Sustainable Energy Reviews*, vol. 151, pp. 111583, 2021. https://doi.org/10.1016/j.rser.2021.111583
[27] V. Andrei, Q. Wang, T. Uekert, S. Bhattacharjee, & E. Reisner, "Solar Panel Technologies for Light-to-Chemical Conversion", *Accounts of Chemical Research*, vol. 55, no. 23, pp. 3376-3386, 2022. https://doi.org/10.1021/acs.accounts.2c00477
[28] F. Polito, G. Huang, & C. Markides, "A Building-Integrated Hybrid Photovoltaic-Thermal (PV-T) Window for Synergistic Light Management, Electricity and Heat Generation", Advanced Science, vol. 12, no. 3, 2024. https://doi.org/10.1002/advs.202408057
[29] E. Tonadi, N. Niharman, & B. Wiranto, "Performance Analysis of Solar Photovoltaic Thermal (PV/T) Dryer for Drying Moringa Leaf", *JTTM Jurnal Terapan Teknik Mesin*, vol. 5, no. 1, 2024. https://doi.org/10.37373/jttm.v5i1.777
[30] J. Zhao, S. Huang, Q. Cai, F. Zeng, & Y. Cai, "Research on Distributed Renewable Energy Power Measurement and Operation Control Based on Cloud-Edge Collaboration", *EAI Endorsed Transactions on Energy Web*, vol. 11, 2024. https://doi.org/10.4108/ew.5520
[31] B. Li, W. Cao, T. Tang, B. Qi, J. Zhao, & C. Liu, "QoS-Based Bi-Level Demand Response for Data Center to Facilitate Renewable Energy Integration", *IEEJ Transactions on Electrical and Electronic Engineering*, vol. 19, no. 5, pp. 625-639, 2024. https://doi.org/10.1002/tee.24024

[32] A. Noppakant and B. Plangklang, "Improving Energy Management through Demand Response Programs for Low-Rise University Buildings", *Sustainability*, vol. 14, no. 21, pp. 14233, 2022. https://doi.org/10.3390/su142114233

[33] M. Abdelghany, A. Al-Durra, & F. Gao, "A Coordinated Optimal Operation of a Grid-Connected Wind-Solar Microgrid Incorporating Hybrid Energy Storage Management Systems", *IEEE Transactions on Sustainable Energy*, vol. 15, no. 1, pp. 39-51, 2024. https://doi.org/10.1109/tste.2023.3263540

[34] K. Singh, A. Chaudhary, & K. Chaudhary, "Three-phase AC-DC Converter for Direct-drive PMSG-based Wind Energy Conversion System", *Journal of Modern Power Systems and Clean Energy*, vol. 11, no. 2, pp. 589-598, 2023. https://doi.org/10.35833/mpce.2022.000060

[35] C. Wang, Q. Zhao, & R. Tian, "Short-Term Wind Power Prediction Based on a Hybrid Markov-Based PSO-BP Neural Network", *Energies*, vol. 16, no. 11, pp. 4282, 2023. https://doi.org/10.3390/en16114282

[36] F. Duan, M. Eslami, M. Khajehzadeh, A. Basem, D. Jasim, & S. Palani, "Optimization of A Photovoltaic/Wind/Battery Energy-based Microgrid in Distribution Network using Machine Learning and Fuzzy Multi-Objective Improved Kepler Optimizer Algorithms", *Scientific Reports*, vol. 14, no. 1, 2024. https://doi.org/10.1038/s41598-024-64234-x

[37] Q. Li, L. Zhang, C. Zhang, Y. Tian, Y. Fan, B. Li et al., "Compact, Robust, and Regulated-Output Hybrid Generators for Magnetic Energy Harvesting and Self-Powered Sensing Applications in Power Transmission Lines", *Energy & Environmental Science*, vol. 17, no. 8, pp. 2787-2799, 2024. https://doi.org/10.1039/d3ee04563c

[38] Q. Zeng, Z. Pan, Q. Zhang, T. Han, W. Zheng, J. Li et al., "CSR Evolution: New Opportunities and Challenges for IoT in Advancing ESG Practices", *International Journal of Frontiers in Engineering Technology*, vol. 6, no. 3, 2024. https://doi.org/10.25236/ijfet.2024.060301

[39] K. Adeusi, A. Adegbola, P. Amajuoyi, M. Adegbola, & L. Benjamin, "The Potential of IoT to Transform Supply Chain Management Through Enhanced Connectivity and Real-Time Data", *World Journal of Advanced Engineering Technology and Sciences*, vol. 12, no. 1, pp. 145-151, 2024. https://doi.org/10.30574/wjaets.2024.12.1.0202

[40] R. Delfianti, V. Tazayul, B. Mustaqim, F. Nusyura, & C. Harsito, "Internet of Things (IoT) Based Electrical Power Monitoring System for Solar Power Plants Using Telegram Application", *Vokasi Unesa Bulletin of Engineering, Technology and Applied Science*, vol. 2, no. 3, pp. 428-443, 2025. https://doi.org/10.26740/vubeta.v2i3.39405

[41] U. Lakhina, N. Badruddin, I. Elamvazuthi, A. Jangra, T. Huy, & J. Guerrero, "An Enhanced Multi-Objective Optimizer for Stochastic Generation Optimization in Islanded Renewable Energy Microgrids", *Mathematics*, vol. 11, no. 9, pp. 2079, 2023. https://doi.org/10.3390/math11092079

[42] M. Wang, H. Gao, D. Pan, X. Sheng, C. Xu, & Q. Wang, "Multi-Energy Load Collaborative Optimization of the Active Building Energy Management Strategy", *Energies*, vol. 17, no. 11, pp. 2569, 2024. https://doi.org/10.3390/en17112569

[43] B. Mahdi, N. Sulaiman, M. Shehab, S. Shafie, H. Hizam, & S. Hassan, "Optimization of Operating Cost and Energy Consumption in a Smart Grid", *IEEE Access*, vol. 12, pp. 18837-18850, 2024. https://doi.org/10.1109/access.2024.3354065

[44] Y. Wang, Z. Yang, X. Zhao, H. Liu, D. Wang, & C. Liu, "Fine-Grained Modeling and Coordinated Scheduling of Source-Load With Energy-Intensive Electro-Fused Magnesium Loads", *IEEE Access*, vol. 12, pp. 47702-47712, 2024. https://doi.org/10.1109/access.2024.3381781

[45] M. Kavindi, K. Amaratunga, E. Ekanayake, A. Fernando, & A. Abesinghe, "CFD Simulation of Airflow Distribution in a Heat Pump-Assisted Deep-Bed Paddy Dryer", *Applied Engineering in Agriculture*, vol. 38, no. 1, pp. 1-8, 2022. https://doi.org/10.13031/aea.14483

[46] B. Li, S. Feng, Q. He, Y. Zhu, Z. Hu, Y. Jiang et al., "Numerical Simulation of Rice Drying Process in a Deep Bed under an Angular Air Duct", *Journal of Food Process Engineering*, vol. 46, no. 12, 2023. https://doi.org/10.1111/jfpe.14438

[47] A. Ahmad, O. Prakash, A. Kumar, R. Chatterjee, S. Sharma, V. Kumar et al., "A Comprehensive State-of-the-Art Review on the Recent Developments in Greenhouse Drying", *Energies*, vol. 15, no. 24, pp. 9493, 2022. https://doi.org/10.3390/en15249493

[48] Z. Chu, Y. Zhao, & Z. Guan, "Simulation and Optimization of Infrared Heating Temperature Field for Heat Shrink Tube Dry Expansion Process", *Journal of Physics: Conference Series*, vol. 2954, no. 1, pp. 012073, 2025. https://doi.org/10.1088/1742-6596/2954/1/012073

[49] T. Gao, X. Han, H. Zhang, Y. Geng, X. Lian, & Z. Fan, "Application of Graded Phase Change Materials for Solar Energy Inter-Seasonal Storage Heating and Thermal Storage Characteristics", *Applied Mathematics and Nonlinear Sciences*, vol. 9, no. 1, 2023. https://doi.org/10.2478/amns.2023.2.00642

[50] M. Kim, A. Han, J. Lee, S. Cho, I. Moon, & J. Na, "Comparison of Derivative-Free Optimization: Energy Optimization of Steam Methane Reforming Process", *International Journal of Energy Research*, vol. 2023, pp. 1-20, 2023. https://doi.org/10.1155/2023/8868540

[51] H. Elqady, G. Sedahmed, & M. Elkady, "Parametric Study for Optimizing Double-Layer Microchannel Heat Sink for Solar Panel Thermal Management", *Scientific Reports*, vol. 12, no. 1, 2022. https://doi.org/10.1038/s41598-022-23061-8

[52] N. Laksmi, M. Mubarok, F. Amaliah, A. Aziz, D. Rahmatullah, D. Herjuno et al., "Design of Automatic Battery Charger Using Forward DC-DC Converter for Solar Home Energy", *Vokasi Unesa Bulletin of Engineering, Technology and Applied Science*, vol. 2, no. 1, pp. 57-66, 2025. https://doi.org/10.26740/vubeta.v2i1.35817
[53] A. Olabi, K. Obaideen, M. Abdelkareem, M. AlMallahi, N. Shehata, A. Alami et al., "Wind Energy Contribution to the Sustainable Development Goals: Case Study on London Array", *Sustainability*, vol. 15, no. 5, pp. 4641, 2023. https://doi.org/10.3390/su15054641
[54] Y. Wang, R. Wang, K. Tanaka, P. Ciais, J. Peñuelas, Y. Balkanski et al., "Accelerating the Energy Transition Towards Photovoltaic and Wind in China", *Nature*, vol. 619, no. 7971, pp. 761-767, 2023. https://doi.org/10.1038/s41586-023-06180-8

BIOGRAPHIES OF AUTHORS

Setiyono Head of Electrical Engineering Laboratory of Gunadarma University Indonesia . Bachelor of Electrical Engineering, 2009. Master of Electrical Engineering in Gunadarma University,2002. Doctor of Information Technology, Gunadarma University Information, 2010.
ID Garuda 1534820
ID Sinta 6687929.
email: setiyono@staff.gunadarma.ac.id.

Elfitrin Syahrul, Bachelor of Electrical Engineering (Universitas Pancasila), 1998. Magister of Electrical Engineering (Universitas Indonesia), 2001. Doctor (Instrumentation et Informatique de l'image – Universite de Bourgogne), 2011.
WoS ResearcherID: JMB-2717-2023

Dyah Nur'ainingsih, Graduated from Gunadarma University, Indonesia, in 1999 with the degree of Bachelor of Electro Engineering. In 2002 graduated with the degree of Master Electrical Engineering from Gunadarma University. Graduated with doctoral degree from University of Gunadarma in 2016. Since 2006 as a Vice Head of Electrical engineering Laboratory in University of Gunadarma.